Reactive Dye Removal by a Novel Biochar/ MgO Nanocomposite

[1]Amna Moazzam, [1]Nadia Jamil, [1]Farah Nadeem, [1]Abdul Qadir, [2]Naveed Ahsan, and [1]Mariam Zameer
[1]*College of Earth and Environmental Science, University of the Punjab, Quaid-e-Azam Campus, Lahore, Pakistan.*
[2]*Institute of Geology, University of the Punjab, Quaid-e-Azam Campus, Lahore, Pakistan.*
ndnaveed@gmail.com*

(Received on 10th May 2016, accepted in revised form 23rd November 2016)

Summary: This research was aimed to synthesize a cost effective charcoal based nano-sorbent and evaluate its adsorption efficiency for the removal of reactive dye blue 221 (RB-221) from synthetic textile waste water. Charcoal was prepared by thermal decomposition of rice straw and a charcoal/MgO nanocomposite was prepared through modified co-precipitation method. The prepared adsorbent was analyzed through X-ray diffraction (XRD), Fourier transform infra-red spectroscopy (FT-IR) and Scanning Electron microscopy (SEM) imaging techniques for its morphology and characterization. XRD analysis showed the crystallite size ranging from 8 to 20 nm. The adsorption efficiency of the nanocomposite was tested through batch experiments. Effects of shaking speed, shaking time, adsorbent dose, pH, temperature and initial adsorbate concentration was studied and optimum conditions were recorded. Langmuir and Freundlich isotherms of adsorption revealed favorable and feasible adsorption of dye on to the charcoal and MgO nanocomposite. Endothermic and spontaneous adsorption was observed through thermodynamic parameters. Data obtained from adsorption studies best fitted pseudo first order kinetic model. The regression factor for this model was calculated to be R^2= 0.887. The results indicate feasible adsorption of RB-221 on nanocomposite of rice straw charcoal/MgO nanocomposite from aqueous solutions.

Keywords: Adsorption, Charcoal, Isotherms, Kinetics, Nanocomposite, Thermodynamics.

Introduction

Most developing countries are located in South East Asian region on the world map. Trans-boundary sharing, rapid industrial development, urbanization and unconventional water management practices have resulted in pollution and scarcity of fresh water resources particularly in this region and generally around the globe [1].

Textile industry is responsible for polluting the environment on largest scale as compared to pollution caused by other industries. According to an estimate, nearly 20% of the effluent that enters in to the water bodies comes from textile processing and manufacturing sector [2]. Dyeing Units make use of large volumes of fresh water as this process includes repeated washing and rinsing. Dyeing of fabric and clothing demands clean and processed water so that salts and minerals do not interfere with the dyes and high color fastness can be achieved. Increasing interest and attraction towards the beauty of colors has resulted in increased demand of dyed stuff [3]. Natural as well as synthetic dyes are used to enhance the physical appearance of white cloth and apparels. When fabric comes in contact with dyes, due to difference of charges not all the dye gets fixed into the fabric resulting in approximately 12-15% of unfixed dyes in the dye bath liquor [4].

Dyes are aromatic compounds and are classified into different types on the basis of difference in the functional and chromophore groups, auxochromes and charge. Chromophore group is the chemical structure that absorbs light in the dye molecule. It is basically a bonded (single and double) electron system. Auxochrome groups act as color enhancers and also increases the affinity of dye molecule towards the structure of fabric [2].

Reactive dyes are the most extensively manufactured dyes in the world. These dyes are also known as azo dyes owing to the presence of one or more azo group (-N=N-) in its chemical structure [5]. According to an estimate, out of all the dyes manufactured synthetically in the world, 20 to 30% are the reactive dyes [6]. To ensure the fixation of dye onto the fibers, electrolytes or buffer solutions are added in the dye bath media. Reactive dyes react chemically with the fiber network of cotton and fix the color in the form of very strong covalent bonds. As a result fibers hold dye molecules very strongly. The fixation ratio of reactive dyes is however 70:30. As compared to all other dyes, 20-30% of the dye remains unfixed and becomes part of the effluent [7].

Effluent discharged from dyeing units contains high concentration mixture of synthetic dyes along with organic and inorganic chemical

*To whom all correspondence should be addressed.

substances [8]. Residual dyes along with considerable amount of metals, chlorides, salts, acids, bases and other reagents when enter into a water body, alters the physical and chemical environment. Colorants make a sheet like covering on the surface of water and hinder the penetration of sunlight and block the oxygen which suffocates the water environment [9].

According to a study, every year around 200,000 tons of spent dye is released into the environment worldwide [10]. In the presence of oxygen, textile dyes particularly reactive dyes undergo incomplete decomposition. Reactive dyes are converted into aromatic amines after decomposition. These amines are very dangerous and responsible for causing cancer in vital organs [9]. Different types of treatments are in practice worldwide to clean textile waste water. The most common treatment methods include physical treatment, chemical treatment, physico-chemical and biological treatment [11].

Removal of textile dyes by adsorption on various chemical and biological materials is a new approach these days. In adsorption, dissolved substances in liquid or gas phase get attached to the surface of adsorbent. Adsorption is applicable where separation and purification is required. In dye removal, due to larger surface area and greater adsorptive capacity, dye molecules and ions get attached to the adsorbent and as a result considerable purification is achieved. Efficiency of the adsorption is directly proportional to the surface area and pore size of the adsorbent [12]. Biochar is the high carbon material with oxygen functional groups and large surface areas obtained by cooking of organic feedstock in the presence of complete or partial supply of oxygen [13,14]. A nanocomposite can be defined as the complex of a definitive crystalline inorganic nonmaterial on any organic amorphous substance. The inorganic material used for activating the organic materials can be one, two, three or even zero in dimensions [15]. The present study involves the use of an eco-friendly and cost effective universal adsorbent *i.e*., biochar as a substrate for making a nanocomposite with magnesium oxide nanoparticles.

Experimental

Preparation of Rice Straw charcoal

Rice Straw was obtained from croplands in university premises and dried under sun. Biochar was prepared by thermal decomposition method. Rice straw was cooked in the absence of oxygen for one and half hour. After that the lid of the container was carefully removed and biochar was allowed to cool. It was then converted into powder form with the help of pestle and mortar. Finely grounded biochar was passed through sieve of 1mm pore size in order to remove any impurity and uncooked material. It was filled in air tight zip lock bags and stored in desiccator to avoid moisture uptake [16].

Synthesis of Nanocomposite

Nanocomposite of Magnesium oxide and rice straw biochar was synthesized by modified co-precipitation method [17]. First of all 10.0g dried and sieved charcoal was dissolved in 100ml of distilled water while continuous stirring. 0.4M solution of $MgCl_2$ was prepared in separate beaker by dissolving 8.132g of hydrated Magnesium Chloride in 100ml distilled water. When the biochar was completely dissolved in the water, $MgCl_2$ solution was added. The solution was kept on stirring for 30 min. 3.2g of sodium hydroxide in the form of pellets were dissolved in the 100ml of distilled water to make 0.8M solution. This solution was added drop wise into $MgCl_2$ and charcoal solution with the help of drip set. Dropping was carried out with continuous stirring through magnetic stirrer. The whole process was carried out at room temperature. After complete dropping, solution was filtered with the help of suction apparatus along with frequent washing with distilled water and ethanol. Precipitates were dried in oven at 150°C for 3 to 4 hours. After complete evaporation of ethanol, nanocomposite was transferred to zip lock bags and stored in the desiccator.

Characterization of Nanocomposite

In order to look into the size, crystallography, shape, structure, orientation and surface area of the prepared nanocomposite of MgO and charcoal, it was characterized through XRD, FTIR and SEM. XRD of the prepared adsorbent was carried out in the range of °2 theta through PANalyticalX'Pert Pro diffractometer. A beam of X-rays was allowed to pass through the sample. This diffraction from the original path was recorded and analyzed according to laws of physics. FTIR analysis of the nanoscale materials was carried out to obtain infrared spectrum of absorption and emission of the nanocomposite. Infrared spectroscopy identifies the functional group that is most active in dye uptake from the textile waste water [18]. SEM was carried out to obtain detailed information about size, porosity and texture of the material [19].

Preparation of the Adsorbate solution

To carry out batch experiments, synthetic sample solutions of known dye concentration were prepared in the laboratory. A stock solution of 1000 mg/L was prepared by dissolving 1.0g dye in 1000ml of distilled water. Standard solutions were prepared from stock by dilution method. Lambda max was calculated for reactive blue 221.

Adsorption Analysis

Number of experiments was carried out to find out the effect of different parameters on adsorptive properties of nanocomposite. Shaking speed, shaking time, adsorbent dose, concentration of adsorbate, pH and temperature were studied for optimization. To carry out the batch experiments, known volume of adsorbate was taken in graduated measuring flasks and selected amount of adsorbent was added into it. Orbital Flask shaker (Vitalflex,made in Koera), hot plate (MSH-20A Wisestir) and pH meter (Escomet RS 232) were used for batch experiments. Conditions were varied for each parameter and results recorded.

Results and Discussion

Outcomes of Nanocomposite characterization

X-Ray Diffraction (XRD)

X-ray diffractogram was recorded at angle 2theta. XRD pattern of charcoal/ MgO nanocomposite indentified 66.5% of periclase (MgO) in the adsorbent. Out of 10 peaks, 4 sharp peaks were identified and matched with the XRD reference pattern for MgO. Since charcoal does not fall under the category of crystalline solids, and contains a lot many carbon containing compounds, 33.4% carbon graphite was identified. 7 short range peaks were clearly visible in the diffractogram that pointed the presence of amorphous substances in the adsorbent. Identified peaks matched with the XRD reference pattern for MgO. Remaining 23.4% peak area appeared to be unidentified. XRD analysis showed the crystallite size of adsorbent to be in the range from 8 to 20 nm. Fig. 1 shows the diffractogram of the reference pattern and synthesized nanocomposite.

Fourier Transform Infrared Spectroscopy (FTIR)

FTIR spectrum with depressions and sharp peaks showed the presence of different functional groups.IR transmittance spectra of the prepared nano-composite were measured in the range from 1000.0 to 4000.0 cm^{-1}. FTIR spectra of the adsorbent show sharp peaks at 3702, 1417, 1022 and 881 cm^{-1}. Each peak indicates the presence of specific functional group involved in the process of adsorption. The peak at 3702 cm^{-1} denotes an OH bond while the peak at 1417 cm^{-1} is attributed to C-C bonding. Bond stretch between Mg-O is denoted by a prominent peak at 1022cm^{-1}. Out of plane bending vibrations were recognized with the sharp peak at 881cm^{-1}.

Scanning Electron Microscopy (SEM)

A focused beam of electron was passed through the powdered sample. Kinetic energy carried by electrons was dissipated through the structure of nanocomposite and different signals were generated. SEM images of the nanocomposite indicate unhomogenized morphology due to the presence of charcoal. The bright region in the images recorded at 100µm denotes the presence of MgO while the dark region indicates the presence of rice straw charcoal. Pore structure was not clearly visible in the electro gram. Fig. 3a and 3b shows the SEM images of charcoal/ MgO nanocomposite.

Outcomes of Adsorption Studies

Adsorption studies were carried out in batch experiments. Parameters affecting the adsorption efficiency were varied one by one while keeping all other conditions constant.

Interaction of Dye Molecules with Adsorbent

FTIR spectra of adsorbent loaded with RB-221 shows 7 bands including five small adsorption bands. Slight depression was noticed at 3345cm^{-1} and a small peak was observed at 1573cm^{-1}. These changes in the pattern were due to the interactions of dye molecules with that of adsorbent. FTIR spectra unloaded and dye loaded nanocomposite is shown in Fig. 2a and 2b.

Effect of Shaking Speed

Known volume and concentration of adsorbate solutions were taken in measuring flasks and shaking speed for RB-221 was varied from 0 to 250 rpm to attain optimum stirring speed. Maximum adsorption for RB-221 was achieved at 200rpm shaking speed with removal efficiency of 68.45% as shown in Fig. 4. The adsorption increases with increase in shaking speed as the resistance between the particles decreases and the dye particles move towards the adsorbent. When all the adsorption sites on the adsorbent get occupied, further uptake is not possible and continuous increase in shaking time initiates the process of desorption.

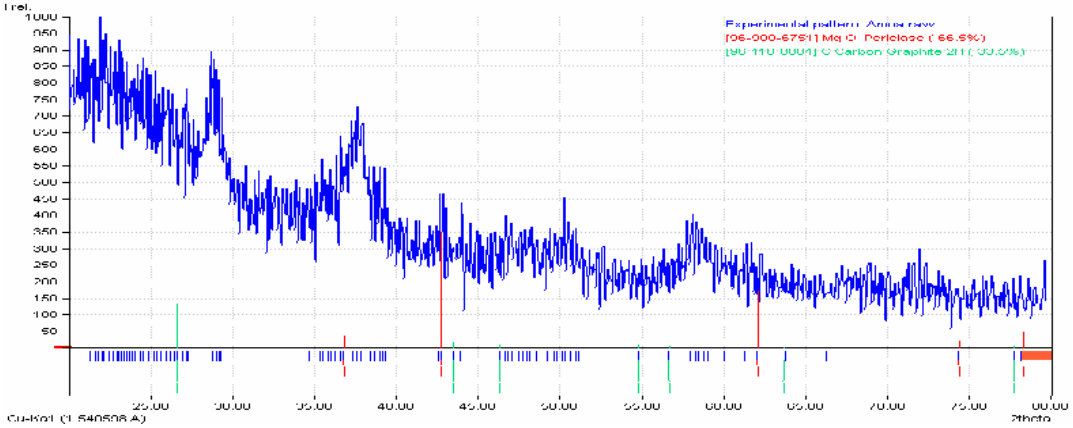

Fig. 1: XRD pattern of rice straw charcoal/ MgO nanoparticles.

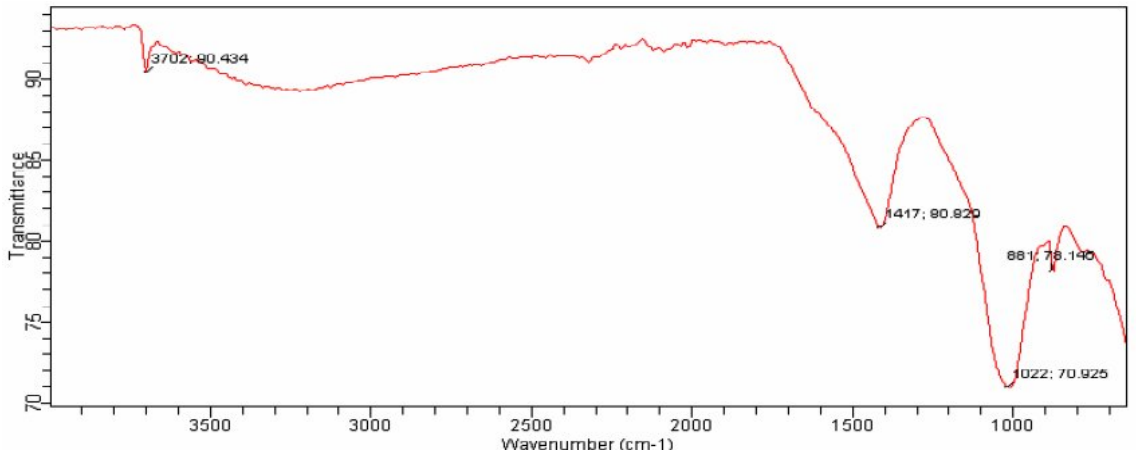

Fig 2a: FTIR spectra of rice straw charcoal/MgO nanoparticles.

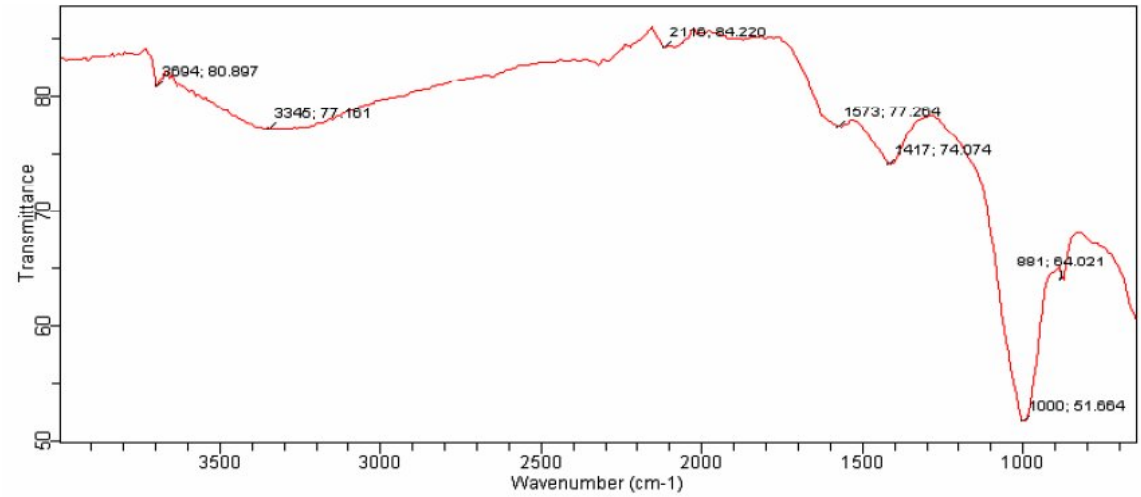

Fig. 2b: FTIR spectra of adsorbent loaded with RY-221.

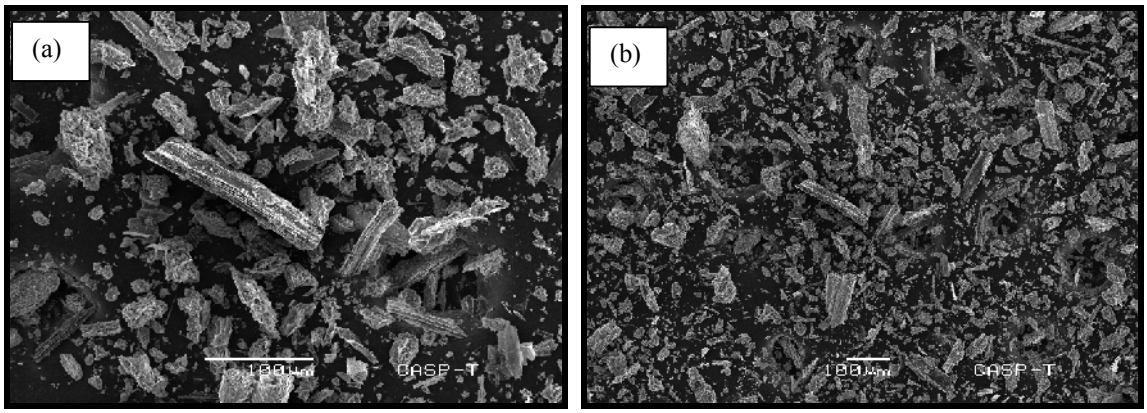

Fig 3 (a, b): SEM images of charcoal / MgO nanoparticles.

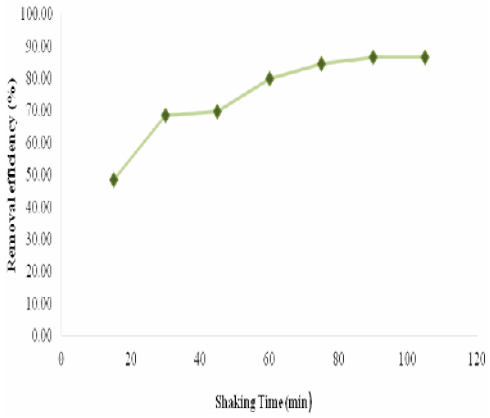

Fig. 4: Graph relating removal efficiency of nanocomposite with varying shaking speed for the removal of RB-221 from aqueous solution.

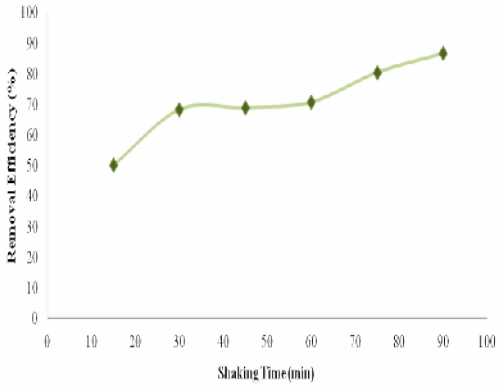

Fig 5: Graph relating removal efficiency of nanocomposite with varying shaking time for the removal of RB-221 from aqueous solution.

Effect of shaking Time

Shaking time was optimized for RB-221 while keeping all other parameters constant. Shaking time was varied from 15 to 90 min at respective optimum shaking speeds for RB-221. Results clearly show rate of adsorption increases with increasing contact time. With reference to the Fig.5, maximum adsorption efficiency of 86.67% for RB-221 was obtained after 90 minutes of shaking. Any further increase in shaking time did not increase or decrease the adsorption.

Effect of Adsorbent Dose

Dose-response relationship was studied by varying adsorbent dose. By keeping all other parameters constant, only adsorbent dose was varied from 0.1g to 0.35g for RB-221. Like shaking time, adsorption also increases with increasing adsorbent dose. Maximum 73.22% removal efficiency for RB-221 was observed with adsorbent dose of 0.35g. The difference in the percentage removal of dyes with 0.3g and 0.35g adsorbent dose was not very large as compared to that recorded with 0.25g that is why 0.25 g was considered as optimum amount of adsorbent as the application of large amounts of adsorbent is not economically feasible at industrial level. At the start of the reaction, number of adsorption sites was less than the amount of dye molecules in the waste water. Later with gradual increase in the adsorbent dose, more of dye molecules bind on the surface of nanocomposite. Directly proportional relationship between adsorption capacity and amount of adsorbent in grams was observed. Fig. 6 shows overall increase in the adsorption efficiency of RB-221 with increase in adsorbent dose.

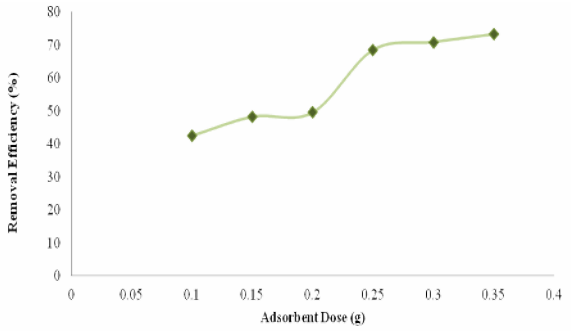

Fig. 6: Graph relating removal efficiency of nanocomposite with varying adsorbent dose for the removal of RB-221 from aqueous solution.

Effect of pH

Batch experiment was conducted in order to study the effect of change in pH on the removal of RB-221. pH was varied from acidic to basic (3,5, 7, 9 and 11) at optimum shaking speed, contact time, adsorbent dose and room temperature. pH was varied with the addition of 1M solution of hydrochloric acid and 1M sodium hydroxide solutions drop wise. Maximum adsorption of 68.45% for reactive blue 221 was obtained at neutral pH. Fig. 7 illustrates the trend of adsorption at different pH conditions.

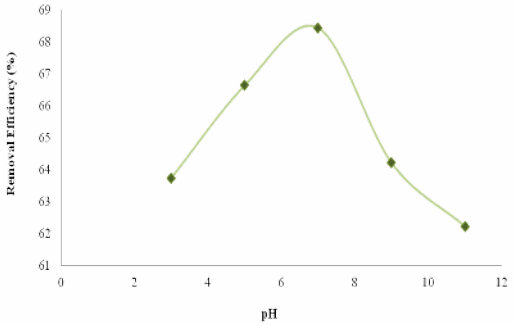

Fig. 7: Graph relating removal efficiency of nanocomposite with varying pH for the removal of RB-221 from aqueous solution.

Effect of Temperature

To find out suitable temperature for maximum removal of RB-221, a batch experiment was carried out at different temperature ranges *i.e.*, 70°, 50°, 30°, 26° (room temperature) and 10°C. Maximum removal was achieved at room temperature. A very slight difference in efficiency of adsorption was observed when temperature was decreased to 50°, 30°and 26°respectively. 77.41% removal was attained at room temperature. Fig. 8 shows the changes in the rate of adsorption in response to the increase and decrease in surrounding temperature.

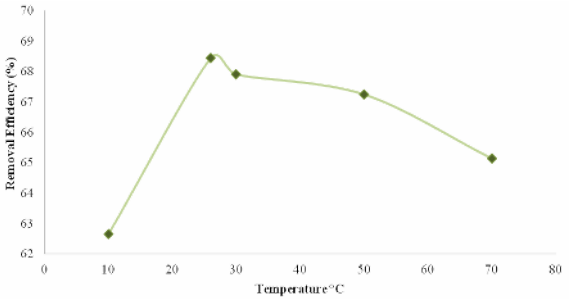

Fig. 8: Graph relating removal efficiency of nanocomposite with varying temperatures for the removal of RB-221 from aqueous solution.

Effect of Concentration of Adsorbate Solutions

In order to optimize concentration of adsorbate solution, batch experiment was executed with increasing the amount of dye in synthetic waste water solution from 30mg/l to 180mg/l. Adsorbent dose, shaking speed and time, pH and temperature were maintained to be optimum. Outcomes of the experiment revealed decrease in percentage removal with increase in concentration of dye in aqueous solution. 90.40% RB-221 was removed from a solution with 30mg/L dye concentration. On the other hand, 62.91% dye was taken by adsorbent from 180mg/L solution as shown in Fig. 9.The number of active sites of the adsorbent are finite and once the adsorbent becomes saturated, no further adsorption takes place. The lesser the dye concentration, the more sites are available for adsorption.

Isotherms of Adsorption

Outcomes of adsorption studies for both the RB-221 were further analyzed through applications of adsorption isotherms.

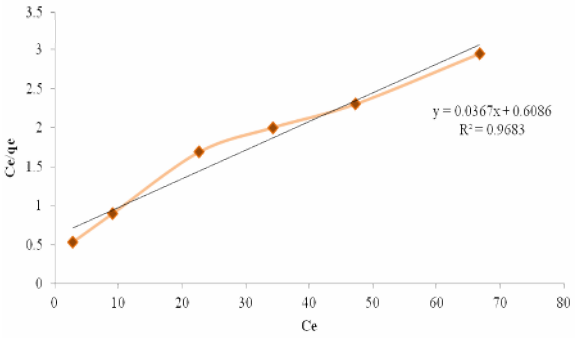

Fig. 9a: Langmuir linear regression fit to the adsorption of RB-221 on Charcoal doped MgO nanoparticles.

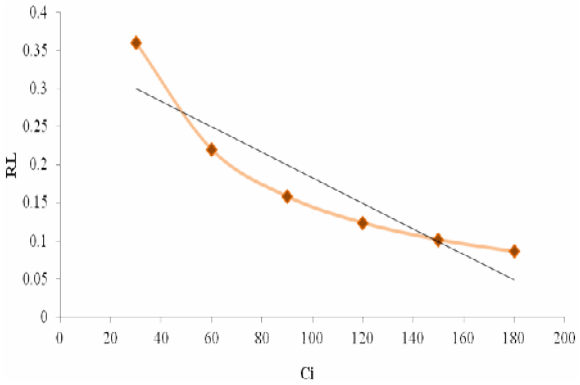

Fig. 9b: Separation factor (R_L) for the adsorption of RB-221 on charcoal/MgO nanoparticles.

Langmuir Isotherm of Adsorption

Langmuir isotherm was applied to adsorption data in order to check for the homogeneity and monolayer adsorption of RB-221 on the surface of charcoal/MgO nanoparticles. The value of coefficient of correlation was determined by linear equation. The value of regression constants pointed that adsorption process followed type-I of Langmuir isotherm. Coefficient of correlation (R^2) and Langmuir maximum adsorption capacity (q_{max}) was found to be q_{max}= 27.77778 mg/g and R^2 = 0.9683 respectively for reactive blue 221. Separation factor (R_L) of Langmuir isotherm was calculated to be between the ranges from 0 to 1 which proves beneficial adsorption. Graphical representation of RB-221 Langmuir isotherm is given in Fig. 9a and b and constants and separation factor for Langmuir isotherms of adsorption for RB-221 are given in Table-1 and 2 respectively.

Table-1: Constants for Langmuir Isotherm of adsorption of RB-221.

Adsorbate	Intercept	q_{max}	Slope	R^2
RB-221	0.608	27.7778	0.036	0.683

Table-2: Langmuir Separation factor for the adsorption of RB-221

Initial Concentration Ci (mg/L)	R_L
30	0.360188
60	0.219652
90	0.158003
120	0.123376
150	0.101198
180	0.085778

Freundlich Isotherm of Adsorption

An empirical model proposed by Freundlich was applied to calculate adsorption intensity of RB-221. Freundlich isotherm was plotted between $\log C_e$ vs log q_e and linear graph was obtained with R^2= 0.9918. Coefficient of correlation indicated favorable adsorption of RB-221 on nano-composite. Freundlich constant (K_f) and "n" was calculated from slope and intercept. Straight line graph is shown in Fig. 10. Constants for Freundlich isotherm of adsorption for RB-221 are given in Table-3.

Table-3: Constants for Freundlich isotherm of adsorption of RB-221.

Adsorbate	Intercept	Slope	K_f	n	R^2
RB-21	0.541	0.451	3.475362	2.217295	0.9918

Thermodynamics of Adsorption

Thermodynamic parameters were applied on the data obtained from adsorption of RB-221 with different temperature conditions. Results of thermodynamic evaluations showed value for Gibbs free energy (ΔG °) in negative and those of enthalpy (ΔH °) and entropy (ΔS °) in positive. Value of ΔG° indicated unprompted nature of adsorption mechanism while positive value of ΔH° pointed out endothermic characteristic of adsorption process. A linear graph was plotted with 1/T on x axis and lnKc on y axis as shown in Fig. 11. This trend indicates high adsorption affinity of dyes towards MgO/charcoal nanocomposite at elevated temperature.

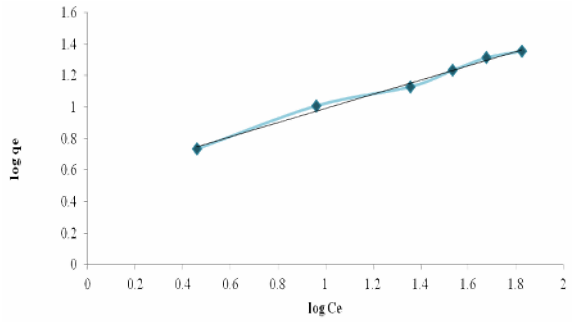

Fig 10: Freundlich linear regression fit to the adsorption of RB-221 on Charcoal/ MgO nanoparticles.

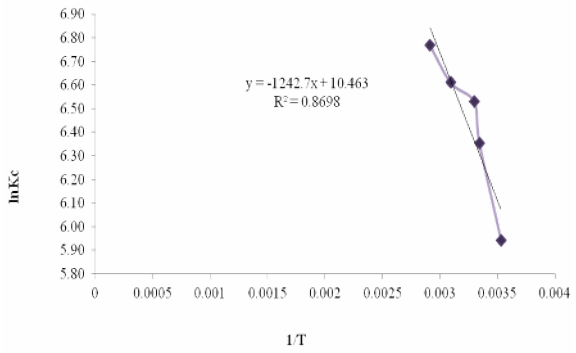

Fig. 11: Graph between 1/T and lnKc of RB-221

Kinetics of Adsorption

Rate of adsorption for both RB-221 was calculated by application of pseudo first order and pseudo second order kinetic models. The regression factor for pseudo first order kinetic model was calculated to be R^2= 0.887. The amount of dye taken up by calculated mass of adsorbent calculated through this model corresponds to the value obtained at equilibrium. On the other hand, dye uptake ($q_{calculated}$) calculated through second order kinetic model does not correspond with the value of dye uptake recorded at equilibrium of adsorption. Data obtained from adsorption studies of RB-221 best fitted pseudo first order kinetic model with good value of coefficient of correlation *i.e*., >10mg/l as shown in Fig. 12. Constants for pseudo first order kinetic equation are given in Table-4.

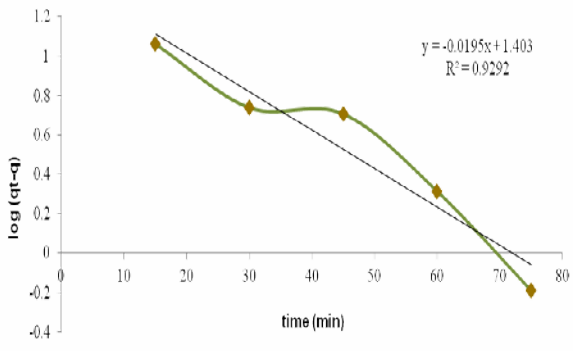

Fig 12: Kinetic equation of pseudo first order on the adsorption of RB-221 on nanocomposite from aqueous solution.

Table-4: Constants for kinetic equation of pseudo first order for the adsorption of RB-221.

Kinetic Parameters	K_1	$q_{experimental}$	$q_{calculated}$	R^2
Pseudo first Order	0.043757	26.0024	25.29298	0.929

Conclusion

The present research work incorporates the synthesis of nano adsorbent for the removal of textile dyes from synthetic waste water. Biochar prepared by thermal decomposition of Rice straw collected from university croplands, was used to prepare a nanocomposite with MgO nanoparticles by modified co-precipitation method. The synthesized nanocomposite was analyzed for surface and morphological studies by XRD, FTIR and SEM. Series of adsorption experiment was carried out to investigate the adsorptive capacity of nanocomposite towards RB-221. All the obtained results confirmed the feasible and beneficial adsorption of reactive blue 221 from synthetic waste water. Use of charcoal makes this nanocomposite cost effective and economically viable. Conversion of organic waste into charcoal reduces the overall waste load on the environment. Replacement of costly and chemical based adsorbents with low cost charcoal based sorbents is highly recommended at industrial scale. MgO/charcoal nanocomposite can be used to decolorize reactive as well as other types of textile dyes from textile industrial effluent.

References

1. I. Khalid, A. Mukhtar and Z. Ahmed, Water Scarcity in South Asia: a Potential Conflict of Future Decades. *J. Polit Stud.,* **21**, 259 (2014).
2. A. Malik and E. Grohmann, (eds.), *Environmental Protection Strategies for Sustainable Development,* Strategies for Sustainability, (1st ed.). Springer Netherlands. (2012), doi: 10.1007/978-94-007-1591-2
3. B. Ratna and S. Padhi, Pollution Due to Synthetic Dyes Toxicity & Carcinogenicity Studies and Remediation. *Int. J. Environ. Sci.,* **3**, 940 (2012).
4. C. Pratum, J. Wongthanate, C. Arunlertaree and B. Prapagdee, Decolorization of Reactive Dyes and Textile Dyeing Effluent by Pleurotus Sajor-Cajo. *Int. J. Integr. Biol*., **11**, 52 (2011).
5. A. Pandey, P. Singh and L. Iyengar, (2007). Bacterial Decolorization and Degradation of Azo Dyes. *Int. Biodeter. Biodegr.,* **59,** 73 (2007).
6. A. Alventosa-deLara, S. Barredo-Damas, M. I. Alcaina-Mirandra and M. I. Iborra-Clar, Ultrafiltration Technology with a Ceramic Membrane for Reactive Dye Removal; Optimization of Membrane Performance. *J. Hazard. Mater.,* **209**, 492 (2012).
7. M. Sumithra and D. Arasi, A Novel Method of Dyeing Nylon 6, 6 with Cold Brand Reactive Dyes and Assessment of its Fastness Properties. *J. Textile. Sci. Eng.,* **2,** (2014).
8. T. Puzyn and M. A. Szlichtyng, Organic Pollutants Ten Years after the Stockholm Convention - Environmental and Analytical Update. (2012).
9. A. Ozturk and M. I. Abdullah, Toxicological Effect of Indole and its Azo Dye Derivatives on Some Microorganisms Under Aerobic Conditions. *Sci. Total Environ,* **358**, 137 (2006).
10. F. M. D. Chequer, G. A. Rodrigues de Oliveira, E. R. A. Ferraz and J. C. Cardoso, Textile Dyes: Dyeing Process and Environmental Impact, Eco-Friendly Textile Dyeing and Finishing. Dr. Melih Gunay (Ed.), InTech, (2013).
11. Z. Carmen and S. Daniela, Textile Organic Dyes – Characteristics, Polluting Effects and Separation/Elimination Procedures from

Industrial Effluents – A Critical Overview. Organic Pollutants Ten Years After the Stockholm Convention - Environmental and Analytical Update. Dr. Tomasz Puzyn (Ed.), InTech, (2012).

12. M. M. A. Latif, A. M. Ibrahim, M. S. Showman and R. R. A. Hamide, Alumina/iron Oxide Nano Composite for Cadmium Ions Removal from Aqueous Solutions. *Inter J. Nonferro Metallurgy*, **2**, 47 (2013).
13. S. P. Sohi, E. Krull, E. Lopez-Capel and R. Bol, A Review of Biochar and its Use and Function in Soil. *Adv. Agron.,* **105**, 47 (2010).
14. R. K. Xu, S. C. Xiao, H. H. Yuan and A. Z. Zhao, Adsorption of Methyl Violet from Aqueous Solutions by the Biochars Derived from Crop Residues. *Bioresour. Technol.,* **102**, 10293 (2011).
15. V. S. A. Kiruba, A. Dakshinamurthy and P. M. Selvakumar, Eco-Friendly Biocidal Silver-Activated Charcoal Nanocomposite: Antimicrobial Application in Water Purification. *Synth. React. Inorg. Me.,* **43**, 1068 (2013).
16. A. Braadbaart, I. Poole, H. D. J. Huisman and B. Van Os, Fuel, Fire and Heat: an Experimental Approach to Highlight the Potential of Studying Ash and Char Remains from Archaeological Contexts. *J. Archaeol. Sci.,* **39**, 836 (2011).
17. T. G. Venkatesha, Y. R. Nayab and B. K. Chethana, Adsorption of Ponceau S from Aqueous Solution by MgO Nanoparticles. *Appl. Surf. Sci.,* **276**, 620 (2013).
18. N. D. Singo, N. A. CheLah, M. R. Jahan and R. Ahmad, (2012). FTIR Studies on Silver-Poly (Methylmethacrylate) Nanocomposites via In-Situ Polymerization Technique. *Int. J. Electrochem. Sci.,* **7**, 5596 (2012).
19. D. McMullan, Scanning Electron Microscopy 1928–1965. *Scanning*, **17**, 175 (2006).